processes

MDPI

Article

Intermittent Optimization of Shale Gas Wells Based on Reservoir–Wellbore Coupling

Yu Fan [1], Jiaxiao Chen [1], Jianhua Xiang [1], Changqing Ye [1] and Guoqing Han [2,*]

[1] Engineering Technology Research Institute, PetroChina Southwest Oil & Gas Field Company, Chengdu 610000, China; fanyu@petrochina.com.cn (Y.F.)
[2] School of Petroleum Engineering, China University of Petroleum Beijing, Beijing 102249, China
* Correspondence: cup_706ac@163.com

Abstract: Shale gas, as an important component of unconventional energy, holds enormous potential value in the energy sector. However, due to the complex geological characteristics and fluid flow mechanisms of shale gas reservoirs, its exploitation faces numerous challenges. This study focuses on the optimization of intermittent production methods for shale gas wells in the Changning block. In this study, a dynamic coordination model of formation recharge and wellhead output was established using real-time pressure monitoring and historical production records as key inputs. Based on this, the dimensionless production efficiency index was optimized by finely regulating the switching timing of the wellhead, thus significantly enhancing the cumulative oil production of the well. The conclusions indicate that the optimization methods proposed in this study can effectively guide the production operations of shale gas wells in the Changning block, thereby enhancing production yield and stability. This research contributes practical value to the field by offering theoretical support and practical guidance for shale gas exploitation, addressing technical challenges in the process.

Keywords: shale gas; intermittent production; optimization; non-dimensional indicator

check for updates

Academic Editors: Qingbang Meng and Chuanliang Yan

Received: 12 May 2024
Revised: 26 June 2024
Accepted: 12 July 2024
Published: 16 January 2025

Citation: Fan, Y.; Chen, J.; Xiang, J.; Ye, C.; Han, G. Intermittent Optimization of Shale Gas Wells Based on Reservoir–Wellbore Coupling. *Processes* **2025**, *13*, 247. https://doi.org/10.3390/pr13010247

Copyright: © 2025 by the authors. Licensee MDPI, Basel, Switzerland. This article is an open access article distributed under the terms and conditions of the Creative Commons Attribution (CC BY) license (https://creativecommons.org/licenses/by/4.0/).

1. Introduction

Shale gas constitutes a crucial component within the realm of unconventional energy resources, harboring significant untapped potential. As attention within the oil and gas sector increasingly gravitates towards unconventional reservoirs, the extraction of shale gas has emerged as a focal point. However, amidst the development process, myriad technical challenges persist due to the unique geological conditions and complex fluid flow mechanisms inherent to shale formations [1,2]. Diverging from conventional reservoir exploitation, shale formations, owing to their tight matrix, confine the majority of gas within impermeable rock layers. Conventional vertical well drilling methods prove inefficient in such scenarios, characterized by low recovery rates, necessitating fracture stimulation techniques to enhance permeability within the pressurized zone, thereby creating regions akin to artificial reservoirs. Concurrently, horizontal drilling techniques are predominantly employed in shale gas development to augment fracture surface area, optimize fracturing efficacy, and elevate extraction efficiencies.

Situated as one of the key focal points for Chinese shale gas development, the Changning block established its shale gas industrial demonstration zone in the Changning–Weiyuan region in 2009, subsequently designated as a national-level shale gas demonstration area of China in 2012. Following these initiatives, efforts were directed towards the development

of shale gas reservoirs within the Changning block, resulting in the accumulation of substantial operational scale and developmental expertise. Notably, certain segments of the shale gas wells within the area have transitioned into the mid-to-late stages of development, necessitating strategic interventions to ensure sustained production and optimize recovery rates. Presently, the primary methodologies for liquid unloading and gas extraction can be broadly classified into two categories: those reliant on artificial lifting mechanisms for energy supplementation and those harnessing natural energy for fluid displacement. As regards wells approaching the later stages of development, artificial energy supplementation predominates, while wells where natural energy suffices for extraction, optimal strategies, balancing developmental costs and environmental considerations, often leverage inherent reservoir energy. Such methodologies encompass intermittent production, selective tubing, foam-assisted displacement, and wellhead depressurization [3–5]. Within the realm of artificial lifting mechanisms, plunger lift systems are prevalent in shale gas wells within the Changning block, whereas intermittent production techniques characterize those relying on natural energy sources.

Intermittent production, a prevalent technique in reservoir development, plays a pivotal role in shale gas exploitation, widely employed both domestically and internationally, particularly within gas reservoirs [2,6]. Take the Sulige and Shenmu gas fields in the Ordos Basin, for example. In the eastern sector of the Sulige gas field, with an average per-well production of 0.5×10^4 m^3/d and a gas–liquid ratio of 0.54 $m^3/10^4$ m^3, approximately 70% of wells fail to achieve critical liquid-carrying capacity as pressure and production decline. Intermittent production is thus implemented to facilitate liquid unloading and gas extraction, relying on sensitivity analysis of casing pressure for individual wells and employing iterative strategies to enhance production for those with heightened sensitivity. While this method effectively boosts well productivity, its applicability is inherently limited, confined to the prevailing production conditions and rendered ineffective post-dynamic reservoir and wellbore system alterations, necessitating periodic scheme recalibrations. The Shenmu gas field, characterized by tight sandstone reservoirs with complex geological attributes and poor reservoir properties, typifies the challenges posed by "low-permeability, low-porosity, and low-pressure" reservoirs. Given the intricate operational framework, discerning well conditions proves challenging. Presently, methods involve computing the optimal pressure recovery timing based on pressure derivative and propagation radius curves. However, this approach is constrained by the sluggish pressure propagation and prolonged recovery time, resulting in excessively protracted shut-in durations.

The Moomba North field in Australia exemplifies the challenges of liquid accumulation during the late stages of production, necessitating a combination of various de-liquefying strategies as the reservoir approaches abandonment pressure. The current approach involves calculating the optimal shut-in flow rate and the critical wellhead pressure to determine the pressure accumulation rate, allowing for control over opening and closing times based on the degree of accumulation. However, this method does not fully exploit the lifting potential provided by annular liquid accumulation pressure [7–9].

In the Changning block under study, the well type is horizontal, with an infill drilling approach, and depths ranging from 4690 to 6865 meters. The formation pressure is between 42 and 67 MPa, while the formation temperature ranges from 87 to 118 °C.

The extraction in this block is conducted through intermittent production. In practice, gas well allocation ranges from 5.3 to 10.3 $\times$ 10^4 m^3/d, with a single well EUR of 0.89 to 1.73 $\times$ 10^8 m^3/d. Daily gas production ranges from 0.4 to 8 $\times$ 10^4 m^3/d, while liquid production ranges from 1 to 8 m^3/d. Considering pressurization, surface design pressure is set between 2 and 3 MPa. Initially, the maximum liquid-to-gas ratio stands at 30 $m^3/10^4$ m^3, gradually diminishing over the production time. The geological makeup of

the rock matrix surrounding a well significantly affects total production, especially in terms of how it responds to stress and its inherent pore structure. Intermittent well start-ups are a strategic method for managing reservoir pressures and optimizing production. At the outset of well operation, high reservoir pressures translate to higher yields. Yet, as operation time extends, the reservoir pressure wanes, causing a corresponding decrease in production. Rational shut-in operations can help to partially restore the reservoir pressure, thereby slowing the rate of production decline and averting a sharp plummet in output to minimal levels.

Presently, the liquid-to-gas ratio ranges from 0.29 to 3 $m^3/10^4$ m^3. The intermittent production scheme employed has become inadequate to meet current production demands, necessitating urgent optimization and theoretical guidance tailored to the characteristics of the studied shale gas well block to devise a new production regime suitable for intermittent production [10].

In this study, we introduce an advanced optimization approach tailored for the intermittent production of gas wells. Through the strategic adjustment of well-switching intervals and a comprehensive analysis of the prevailing production dynamics, our method offers a robust scientific framework aimed at enhancing gas recovery rates and minimizing the necessity for liquid unloading interventions. This method precisely calculates the supplied reservoir fluids parameters such as pressure, flow rate, and liquid holdup along the wellbore. It establishes mathematical models for performing system optimization and rapid response recommendations through parameter sensitivity analysis.

2. Theoretical Models

In the context of our theoretical model, we have delineated the intermittent production process into three distinct phases: the "gas well IPR prediction model based on wellhead test data analysis", the "dynamic model for the shut-in and flowback phase", and the "wellbore flow model during the liquid-lifting phase". Building upon these foundational stages, and considering reservoir effects, we have further developed a "reservoir–wellbore coupled model for the production phase". This model integrates the analysis of flow patterns that correspond to the fluid characteristics at each stage within the wellbore. By applying conservation equations, we effectively couple the state variables across these stages, thus capturing the comprehensive flow dynamics of intermittent production.

2.1. Gas Well IPR Prediction Model Based on Wellhead Test Data Analysis

Combining intermittent production well pressure recovery patterns with the principles of reservoir fluid mechanics, the optimal shut-in time and degree of restoration are determined based on the gas well productivity equation [11,12]. The radial flow steady-state gas deliverability equation governs the stable gas flow dynamics.

$$q_{\mathrm{sc}} = \frac{774.6kh}{\ln \frac{r_{\mathrm{i}}}{r_{\mathrm{w}}} \mu \overline{ZT}} (p_{\mathrm{R}}^2 - p_{\mathrm{wf}}^2) \tag{1}$$

where q_{sc} is the formation deliverability, m^3/d; P_{wf} is the bottom-hole flowing pressure, MPa; p_R is the mean reservoir pressure, MPa; μ is the gas viscosity, mPa·s; Z is the gas deviation factor, dimensionless; T is the bottom-hole temperature, K; k is the permeability, 10^{-3} μm; h is the reservoir thickness, m; r_i is the gas drainage radius, m; and r_w is the wellbore radius, m.

The value of 774.6 is a coefficient derived from standard conditions and unit conversion. It can be deduced from Darcy's productivity formula: $q = 2\pi rhk/\mu \times dp/dr$. At this point, the unit of q is m^3/s. According to the gas state equation, one can obtain $q = q_{sc}P_{sc}ZT/(PZ_{sc}T_{sc})$. By combining these two for-

mulas, one can derive $\pi T_{sc}Z_{sc}/P_{sc}/q_{sc} \times kh/(\mu TZ) \times 2pdp = dr/r$. For standard conditions, take T_{sc} = 293 K, P_{sc} = 0.101325 MPa, and Z = 0.976. Also, the unit of q_{sc} is converted to m^3/d, so the coefficient is multiplied by $86{,}400/10^6$. This results in $774.6 \approx 3.149 \times 293 \times 0.976/0.101325 \times 86{,}400/10^6$.

By taking the derivative of the above formula, we obtain (2) and (3):

$$\frac{dp_R^2}{dr_i} = \frac{d\left(\frac{\mu\overline{ZT}q_{sc}}{774.6kh}\ln\frac{r_i}{r_w}\right)}{dr} \tag{2}$$

$$\frac{dp_R}{dr_i} = \left(\frac{\mu\overline{ZT}q_{sc}}{774.6Kh}\cdot\frac{\ln\frac{1}{r_w}}{2p_R}\right)\frac{1}{r_i} \tag{3}$$

Based on the established relationship between the pressure propagation radius and pressure, we differentiate to plot the curve of the pressure derivative against the radius. The tangent lines at the early and late stages of the pressure derivative intersect to determine the optimal restoration time [13].

Considering the well conditions of a mid-to-deep shale gas well, conventional exponential and binomial productivity equations fail to fit the reservoir gas IPR curve [14–16]. Therefore, a modified single-phase exponential productivity equation is employed to describe this well's characteristics.

The original wellhead test data contain noise and missing values, necessitating further cleaning and processing as a basis for adjustment factors [17,18]. The following function is used to fit and smooth the test pressure data for analysis:

$$y = n_1 + n_2x + n_3x^{0.5} + n_4\exp(-x) \tag{4}$$

We have developed a function grounded in empirical formulas that describe the pressure characteristics of the tubing and casing. This function utilizes actual wellhead test data to generate oil casing pressure–time curves. By treating time as the independent variable (x-axis) and pressure as the dependent variable (y-axis), we apply the least squares fitting method to derive the relationship. The resulting empirical coefficients, denoted as n_1, n_2, n_3, and n_4, are then employed to compute a smoothed pressure curve that corresponds to uniformly distributed time inputs. Using wellhead test data as a reference for calibration, we have incorporated a water saturation change factor, denoted as γ, to quantify the alterations in formation fluid influx near the wellbore. This adjustment is achieved by introducing additional fitting coefficients c. The factor γ is correlated with the wellbore flow pressure and can be mathematically expressed as follows [17]:

$$\gamma = \left(e^{1/c_1+c_2ln(p_{wf})+c_3p_{wf}}\right)^{c_4} \tag{5}$$

Combining the exponential deliverability equation with γ, the reservoir's IPR curve is obtained as follows:

$$q_{sc} = \frac{774.6kh(p_R^2 - p_{wf}^2)}{\mu\overline{ZT}\ln\frac{r_i}{r_w}}\gamma \tag{6}$$

The deliverability equation is established based on a two-phase modification of the conventional exponential equation, wherein the unknown parameters are obtained through fitting to actual wellhead data curves. Genetic algorithms are employed to automatically fit the original data to the equation, yielding the fitting parameters.

$$q_{sc} = \frac{774.6kh(p_R^2 - p_{wf}^2)}{\mu\overline{ZT}\ln\frac{r_i}{r_w}}\left(e^{1/c_1+c_2ln(p_{wf})+c_3p_{wf}}\right)^{c_4} \tag{7}$$

Figure 1 illustrates the measured data extracted from the well tests, alongside the inflow performance relationship (IPR) curve derived from the regression analysis using our refined capacity equation (Equation (7)). This dataset, specific to the Changning block, is further elaborated in the subsequent Section 3. The yellow-shaded region delineates the regression envelope, encompassing scattered data points that signify the variability in the measurements. The breadth of this area indicates the potential variability in values. Utilizing this IPR curve, we conduct an analysis to determine the formation supply capacity corresponding to various bottom-hole flow pressures.

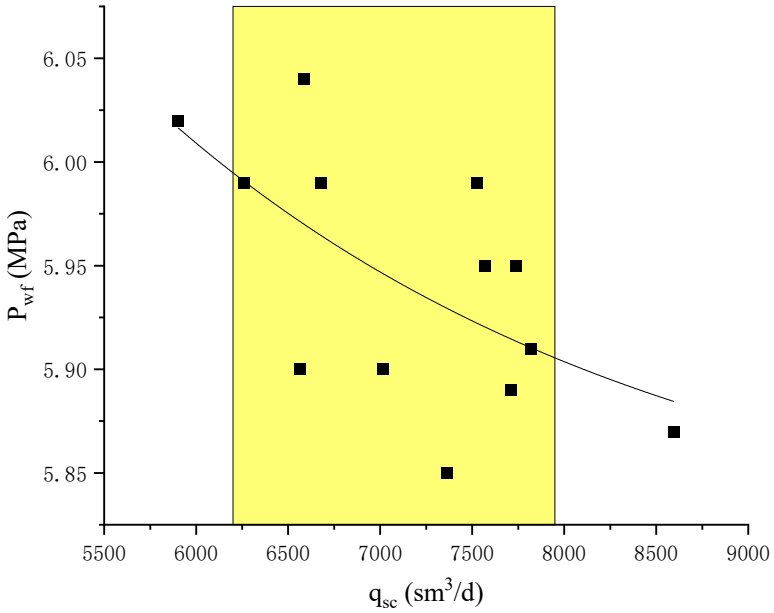


Figure 1. Comparison between IPR curve prediction results and actual results.

2.2. Dynamic Model for Shut-In and Flowback Phase

According to the ideal gas state equation, the pressure formulas for the tubing and casing can be expressed as follows:

$$P_c V_{cg} = \frac{Z_c R T_c}{M} m_{cg} \tag{8}$$

$$P_t V_{tg} = \frac{Z_t R T_t}{M} m_{tg} \tag{9}$$

where P_c is the casing pressure, MPa; V_{cg} is the volume of air in the annulus, m^3; Z_c is the gas deviation factor at a given temperature and pressure in the annulus (this value can be calculated from the SRK equation); m_{cg} is the mass of the gas in the annulus, kg; M is the molar mass of gas, mol/kg; R is the gas constant, J/(mol·K); and T_c is the temperature in the annulus, °C. The subscript c means the tubing-casing annulus, and t means tubing.

The gravity equation of the air column is [19,20]

$$P_{cwu} = P_c \exp\left(\frac{0.03148 \gamma_g h_{cg}}{T_c Z_c}\right) \tag{10}$$

$$P_{twu} = P_t \exp\left(\frac{0.03148 \gamma_g h_{tg}}{T_t Z_t}\right) \tag{11}$$

where P_{cwu} is the pressure at the surface of the liquid in the tubing-casing annulus, MPa; γ_g is the relative density of gas; and h_{cg} is the height of gas column in the tubing-casing annulus, m.

The gravity equation of the liquid column is

$$P_{cw} = \rho_w g h_{cw} \tag{12}$$

$$P_{tw} = \rho_w g h_{tw} \tag{13}$$

where P_{cw} is the pressure drop of the liquid in the annulus, MPa; and h_{cw} is the height of the liquid in the tubing-casing annulus, m.

Given the ongoing fluctuations in pressure and the interconnection between the casing and the tubing bottom, it is evident that their pressures are in equilibrium. This consistent pressure state underscores the fundamental principle that the pressures at these two critical points within the well are inherently equal.

$$P_{cwu} + P_{cw} = P_x = P_{twu} + P_{tw} \tag{14}$$

$$P'_{cwu} + P'_{cw} = P'_x = P'_{twu} + P'_{tw} \tag{15}$$

where P_x is the pressure of the casing shoe, MPa.

Initial condition:

$$h_{cw} = 0 \tag{16}$$

Due to the use of tubing production in the well opening process, it is reasonable to assume that the fluid level in the annulus is zero when shut in. Consequently, the height of the tubing fluid level can be calculated using Equation (14).

Auxiliary equation:

$$V_{cg} = A_t h_{cg} \tag{17}$$

$$V_{tg} = A_t h_{tg} \tag{18}$$

$$h_s = h_{cg} + h_{cw} \tag{19}$$

$$h_s = h_{tg} + h_{tw} \tag{20}$$

$$\Delta m_{cw} = m'_{cg} - m_{cg} \tag{21}$$

$$\Delta m_{tg} = m'_{tg} - m_{tg} \tag{22}$$

$$\Delta m_{cw} = m'_{cw} - m_{cw} \tag{23}$$

$$\Delta m_{tw} = m'_{tw} - m_{tw} \tag{24}$$

$$\Delta m_g = \Delta m_{tg} + \Delta m_{cg} \tag{25}$$

$$\Delta m_w = \Delta m_{tw} + \Delta m_{cw} \tag{26}$$

$$\frac{\Delta V_w}{\Delta V_g} = \frac{\Delta m_w \rho_{gsc}}{\Delta m_g \rho_w} = LGR \tag{27}$$

where V_{cg} is the volume of gas in the annulus, m^3; h_s is the height of tubing, m; Δm_{cg} is the mass change of air mass in the tubing-casing annulus, kg; Δm_c is the change in mass of the total gas, kg; ΔV_w is the volume of liquid that injected into the formation, m^3; ΔV_g is the volume of gas that injected into the formation, m^3; LGR is the liquid–gas ratio, m^3/m^3; and ρ_{gsc} is the gas density in the standard condition, kg/m^3.

Figure 2 shows the model of the tubing and casing profile used to establish the above theoretical equation. The blue arrow indicates the supply of fluid from the formation at the bottom of the wellbore.

Upon the foundation of the previously established formulae, a simplified set of equations is derived, enabling the solution of six unknowns: the liquid levels within the tubing and the tubing-casing annulus, along with the mass of the gas and liquid phases.

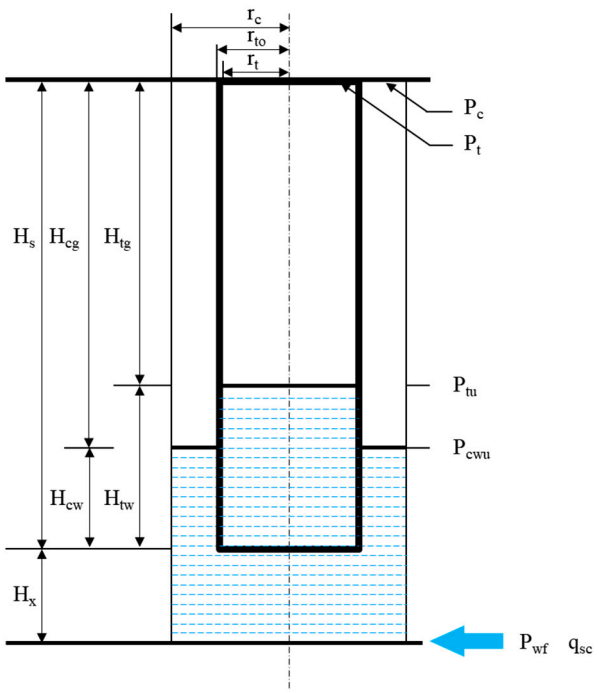


Figure 2. Dynamic model diagram of shut-in flow phase.

Based on Equation (8), an equation for the tubing-casing annulus can be established:

$$\frac{P'_c V'_{cg}}{P_c V_{cg}} = \frac{Z'_c(m_{cg} + \Delta m_{cg})}{Z_c m_{cg}} = \frac{P'_c h'_{cg}}{P_c h_{cg}} \tag{28}$$

The increase in gas mass within the tubing is directly correlated with the gas column height in the annulus; similarly, an equation can be established:

$$\frac{P'_t V'_{tg}}{P_t V_{tg}} = \frac{Z'_t(m_{tg} + \Delta m_{tg})}{Z_t m_{tg}} = \frac{P'_t h'_{tg}}{P_t h_{tg}} \tag{29}$$

The equation of liquid mass increment Δm_{cw} and Δm_{tw} is established:

$$\Delta m_{cw} = \rho_w A_c (h'_{cw} - h_{cw}) \tag{30}$$

$$\Delta m_{tw} = \rho_w A_t (h'_{tw} - h_{tw}) \tag{31}$$

According to the liquid–gas ratio relationship, the equation of Δm_w is established:

$$\Delta m_w = LGR \frac{\rho_w}{\rho_{gsc}} \Delta m_g \tag{32}$$

The equation for the mass of gas inflow into the wellbore over a designated time interval (dt) is established:

$$\Delta m_g = q_{sc} * dt * \rho_g \tag{33}$$

where dt is the time step, s; and ρ_g is the density of the current position under current temperature and pressure conditions, kg/m^3.

Substitute Equations (17) and (18) into Equation (15).

$$P'_{cwu}(h'_{cw}) + P'_{cw}(h'_{cw}) = P'_{twu}(h'_{tw}) + P'_{tw}(h'_{tw}) \tag{34}$$

In summary, by examining the curves of P_c and P_t over time, along with the initial state at h_{cw}, it is feasible to determine h'_{cw} and h'_{cw}, consequently deriving the variations in mass of oil and gas within the annulus between two time steps. The dynamic model established herein facilitates the depiction of temporal variations in pressure parameters within the casing, as illustrated in Figures 3 and 4.

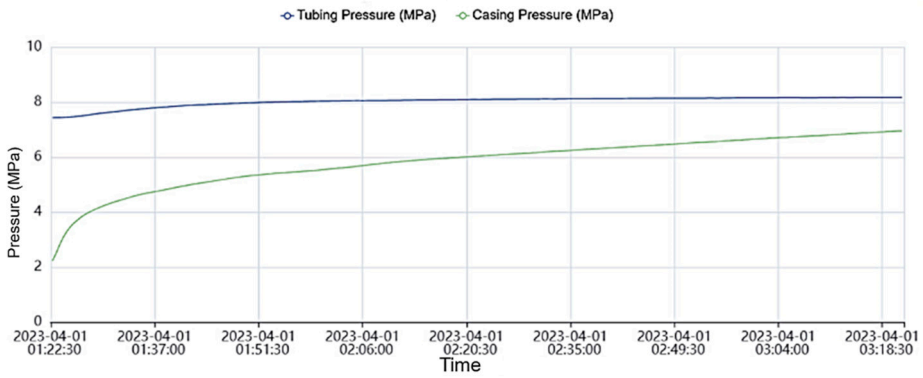


Figure 3. Curve of raw casing pressure over time during shut-in.

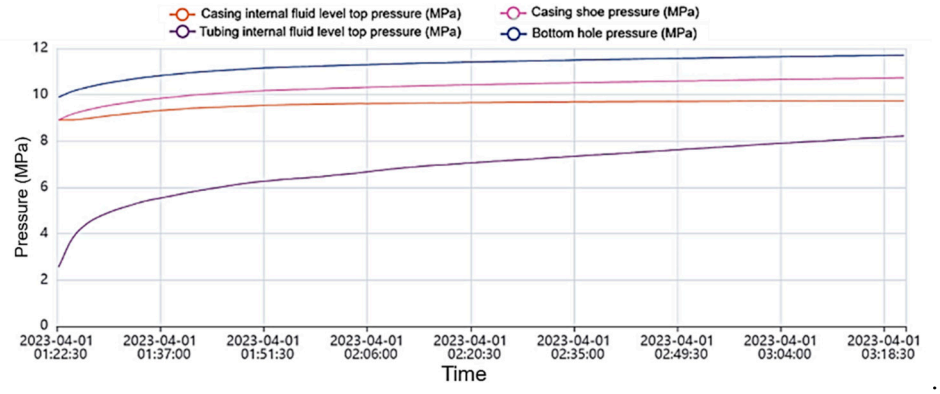


Figure 4. Pressure curve during shut-in period.

2.3. Wellbore Flow Model for Fluid Lifting Phase

The flowing situation in the wellbore at the fluid lifting phase is shown at Figure 5.

The casing pressure calculations at the casing shoe can be utilized to forecast gas–liquid production rates. Q_g is the gas production, m^3/d; $\widetilde{Q_g}$ is the calculated gas production, m^3/d; Q_w is the water production, m^3/d; $\widetilde{Q_w}$ is the calculated water production, m^3/d. The gas production rates of the wellhead can be calculated by employing a cyclic iterative computation method, as depicted in Figure 6. To enhance the accuracy and reliability of our predictions, we must address the following key technical challenges:

(a) Liquid level height determination: Accurate computation of the liquid level height within the annulus is essential. We need to establish a method that reliably measures this parameter, which significantly affects the production dynamics.
(b) Downstream pressure calculation: The calculation of downstream pressure is crucial for understanding the flow behavior in the well system. We must refine our approach to ensure the precision of this calculation.
(c) Pressure boundary condition convergence: Achieving convergence in the pressure boundary conditions is vital for the stability of our computational model. We must develop techniques that ensure the model's robustness under diverse operational scenarios.

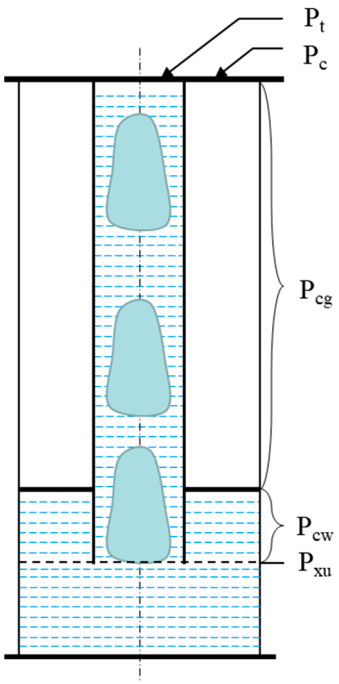


Figure 5. Gas–liquid distribution diagram during well opening.

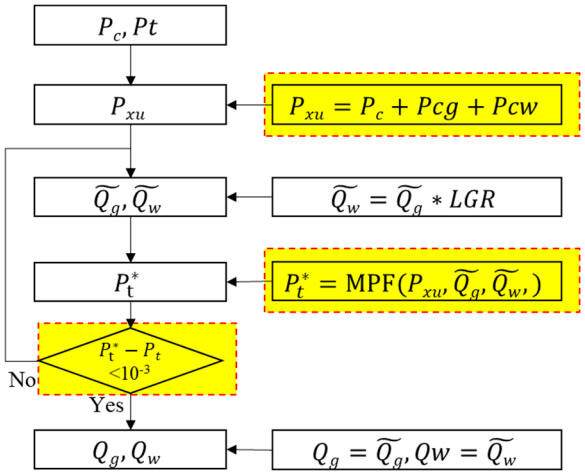


Figure 6. Iterative calculation flow.

When liquid is present in the annular space, the flow of high-pressure gas is impeded, maintaining a constant gas mass. As the liquid level descends, the annular pressure drops sharply. The deceleration in the rate of pressure decrease at the point where the liquid level reaches zero marks a critical juncture. Beyond this point, the gas mass gradually diminishes, and the rate of pressure decline slows. The pressure curve exhibits a distinct transition from a steep descent to a more gradual decline. This critical moment is referred to as the "elbow point" in the curve's profile.

To pinpoint the elbow points along the pressure curve, we conduct a residual analysis. This process entails comparing the observed data points with those predicted by the fitted model to calculate the residuals. The elbow points, which correspond to significant changes in the curve's slope, are characterized by the most pronounced peaks in these residuals. The approach to identifying these inflection points is as follows:

(1) For a given dataset, a linear model is fitted to derive the curve of best fit.

(2) Residuals, representing the perpendicular distances between data points and the fitted curve, are computed.
(3) Elbow points are pinpointed based on fluctuations in residuals, with particular attention to maximal jumps.
(4) The positions of the identified elbow points along with their corresponding residual values are returned.

Utilizing the elbow point recognition method, we identify the time point at which the annular liquid level reaches zero, denoted as t_{elbow}, facilitating the computation of the annular liquid level at any given time. Given the proximity of data collection intervals to this stage, the annular liquid level at any arbitrary time during this phase is treated as varying linearly.

When $t_{open} \leq t \leq t_{elbow}$:

$$h_{cw}(t) = h_{cw_open} - \frac{h_{cw_open}(t - t_{open})}{t_{elbow} - t_{open}} \tag{35}$$

When $t > t_{elbow}$:

$$h_{cw}(t) = 0 \tag{36}$$

The downstream pressure calculation method is established as follows:

(1) Dividing the pipeline trajectory into elemental segments, the downstream pressure is computed segment by segment.
(2) Assuming the downstream pressure, the average pressure and temperature are calculated.
(3) The thermophysical properties under the current pressure and temperature conditions are determined.
(4) The pressure drop within the pipeline is computed based on the segment length and pressure gradient.
(5) The downstream pressure of the segment is then calculated.
(6) In case of a significant deviation between the computed value and the assumed value, an iterative strategy is employed to update the downstream pressure.
(7) Setting this pressure as the upstream pressure for the next segment, the calculation process is iteratively repeated until the final segment is reached.

In the acquisition of pressure boundary conditions, each flow rate corresponds to a specific tubing pressure, yet identical tubing pressures may correspond to multiple flow rates. Under a fixed liquid production rate, as gas production increases, gravitational pressure drop predominates initially, resulting in a decrease in wellbore pressure and subsequent rise in wellhead pressure. However, with further increases in gas production, the significant rise in high-velocity gas enhances the frictional pressure drop, thereby introducing multi-solution scenarios and rendering the calculation process non-convergent. Figure 7 demonstrates the multi-solutions of wellhead pressure corresponding to various gas production rates given a constant bottom-hole pressure. This phenomenon underscores the requirement for our model to autonomously perform sophisticated analyses to pinpoint the challenges associated with determining the appropriate gas production rate under a specified wellhead pressure.

To address the multi-solution nature of flow rates and pressures, a convergence method for pressure boundary conditions is proposed. Utilizing the nearest neighboring daily production rate as the initial value, a greedy algorithm is employed to calculate the closest neighboring production rate, thereby circumventing non-convergence issues encountered in multiphase flow within the pipeline. The algorithmic procedure is delineated in Figure 8.

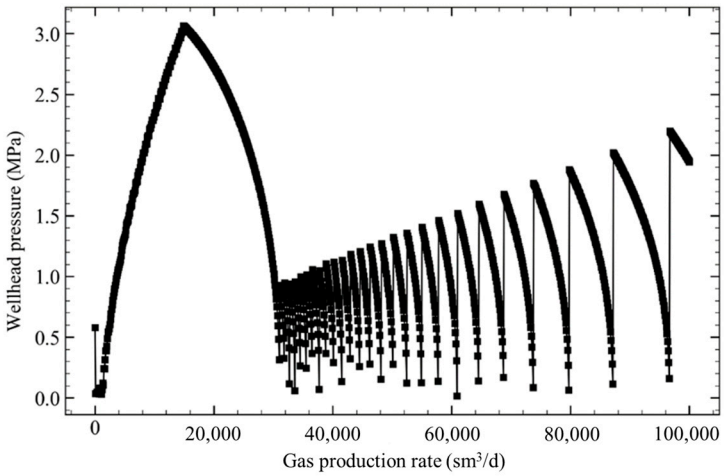


Figure 7. Multi-solvability of flow rates and wellhead pressures.

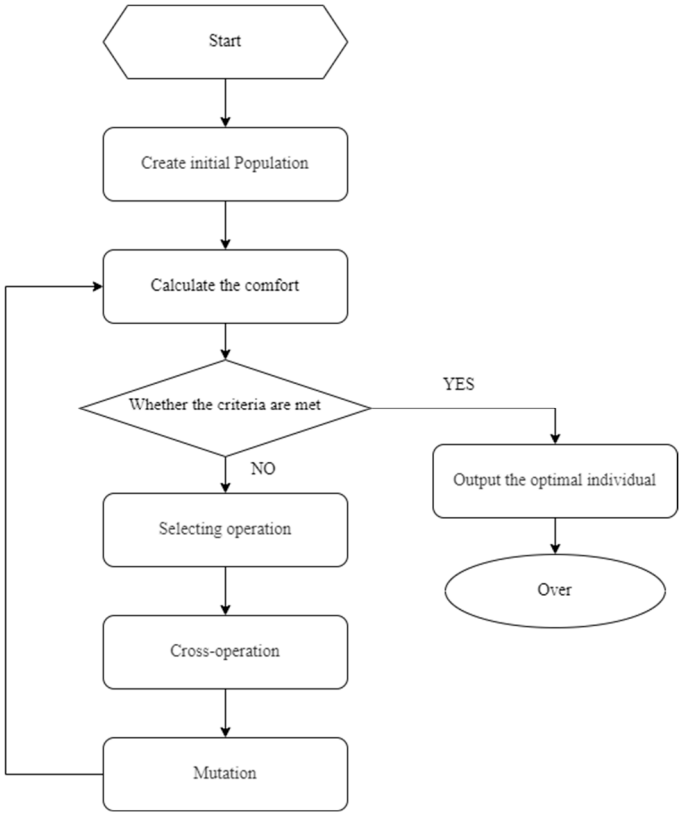


Figure 8. Flow chart of convergence algorithm for pressure boundary conditions.

2.4. Reservoir–Wellbore Coupling Model for Production Phase

During well production, subsurface fluids flow from the reservoir into the wellbore, facilitating extraction. Throughout this process, the reservoir's energy output to the wellbore significantly influences reservoir behavior. The complex interplay between the wellbore and the reservoir highlights the importance of developing a comprehensive coupled model. This model is built upon three key theoretical components previously discussed:

A gas well inflow performance relationship (IPR) prediction model, which is based on an analysis of wellhead test data.

A dynamic model that addresses the shut-in and flowback phase of operations.

A wellbore flow model that is specifically tailored for the fluid lifting phase.

We begin with the assumption of a uniform pressure distribution across the gas reservoir before production starts, represented by an initial pressure P_0. During the early stages of production, which is a relatively short period, the pressure at the reservoir boundaries is generally considered to have a minor impact on the gas well's production performance.

Furthermore, it is assumed that the bottom-hole flowing pressure remains constant throughout the production process.

$$\begin{cases} p(r,t)|_{t=0} = p_0 \\ p(r,t)\Big|_{r=r_W} = p_{wf} \end{cases} \tag{37}$$

According to the above boundary conditions, using the Duhamel principle, we assume a constant bottom-hole flowing pressure. Under this assumption, the relationship between the pseudo-pressure drop Δm_{wfc} induced by production at a constant bottom-hole flowing pressure and the constant unit production rate Δm_{wfur} can be expressed as

$$\Delta m_{wf,cp}(t) = \int_0^t q(\tau)\Delta m'_{wf,ur}(t-\tau)d\tau \tag{38}$$

The equations for Δm_{wfc} and Δm_{wfur} in Equation (38) are shown below:

$$\begin{aligned} \Delta m'_{wf,ur}(t) &= \frac{\partial\left(\Delta\Psi'_{wf,ur}(t)\right)}{\partial t}(t) \\ \Delta m_{wf} &= m(p_i) - m(p_{wf}) \end{aligned} \tag{39}$$

A Laplace transform is applied to the above formula to obtain the production rate $\overline{q}(s)$ and cumulative production $\overline{Q}(s)$.

$$\overline{q}(s) = \frac{\Delta m_{wf,cp}}{s^2 \Delta \overline{m}_{wf,ur}} \tag{40}$$

$$\overline{Q}(s) = \frac{\overline{q}(s)}{s} \tag{41}$$

$$\Delta m_{wf,cp} = \frac{1}{\mu Z}(p_i^2 - p_{wf}^2) \tag{42}$$

The Stehfest algorithm is used for numerical inversion of the above formula to convert the numerical solution to the real time domain.

$$\begin{aligned} &\Delta\overline{m}_{wf,ur} = \tfrac{1422T}{khs} \\ &\left\{\tfrac{I_0(\alpha r_w)K_1(\alpha r_e)+I_1(\alpha r_e)K_0(\alpha r_w)}{\alpha r_w[I_1(\alpha r_e)K_1(\alpha r_w)-I_1(\alpha r_2)K_1(\alpha r_e)]} + S\right\} \end{aligned} \tag{43}$$

where I_0, K_0, I_1, K_1 are the modified Seibel function.

The equations for α and η in Equation (43) are shown below:

$$\alpha = \sqrt{s/\eta} \tag{44}$$

$$\eta = \frac{2.637 \times 10^{-4} k}{\varphi(c\mu)_{avg}} \tag{45}$$

When the reservoir is not affected by the boundary, $\Delta\overline{m}_{wf,ur}$ can be expressed as

$$\Delta\overline{m}_{wf,ur} = \frac{1422T}{khs}\left[\frac{K_0(\alpha r_w)}{\alpha r_w K_1(\alpha r_w)} + S\right] \tag{46}$$

For the Laplace transform Stehfest algorithm, the numerical inversion formula is as follows, assuming that the Laplace transform of the function $f(t)$ is $\overline{f}(s)$.

$$\overline{f}(s) = L[f(t)] = \int_0^\infty f(t)e^{-st}dt \tag{47}$$

The function $f(t)$ can be expressed when $t = T$.

$$f(T) = \frac{\ln 2}{T}\sum_{i=1}^{N} V_i\overline{f}(\frac{\ln 2}{T}i) \tag{48}$$

V_l in Equation (48) can be expressed as

$$V_l = (-1)^{\frac{N}{2}+i}\sum_{k=\frac{i+1}{2}}^{min(t,\frac{N}{2})} \frac{k^{\frac{N}{2}}(2k)!}{(\frac{N}{2}-k)!k!(k-1)!(i-k)!(2k-i)!} \tag{49}$$

We can integrate the distinct phases of the wellbore's control volume and control surface into a cohesive model by employing the principles of mass conservation and continuous pressure behavior as governing constraints. This methodology enables the incorporation of diverse influential factors, such as the gas–liquid ratio, as tunable input parameters. The integrated model's output is sensitive to adjustments in these parameters, providing a dynamic assessment of how they interact and affect overall well performance.

$$\frac{d}{dt}\int_{cv}\rho dV + \int_{cs}\rho(\mathbf{v_r}\cdot\mathbf{n})dA = 0 \tag{50}$$

In this context, $\mathbf{v_r}$ denotes the relative velocity of the fluid with respect to the control surface (m/s). The symbol n represents a unit normal vector to the control surface, which is a dimensionless quantity.

Using individual time intervals as the fundamental units, cumulative production over an extended duration is computed via integration. Each segment, delineated by the onset and cessation of well operations, encapsulates a distinct temporal unit wherein production accrues.

$$Q(t) = \int_{t_0}^{t_1} q(t)dt \tag{51}$$

where t_0 is the time of opening the well, and t_1 is the time of shut-in.

Subsequently, integrating these segments over the entire temporal span yields the aggregate production over the designated period.

$$\begin{aligned} N_p &= \sum_{i=1}^{k} Q_i \\ N_p &= \int_0^t Q(t)dt \end{aligned} \tag{52}$$

$k = 1, 2, \cdots, n-1, n$.

3. Result and Discussion

Using a time-coupled model, iterations are performed to determine the instantaneous production rate, as illustrated in Figure 8. Initially, the various components of the system are interconnected to ensure an accurate simulation reflecting their interactions. Subsequently, time is discretized into small time increments, and within each increment, the system's state

is updated, accounting for various influencing factors. Through continuous iteration and updating, the instantaneous production rate at different time points is computed, thereby enhancing the understanding of the system's dynamic behavior. Employing a wellhead model enables real-time calculation of gas production, as depicted in Figure 9.

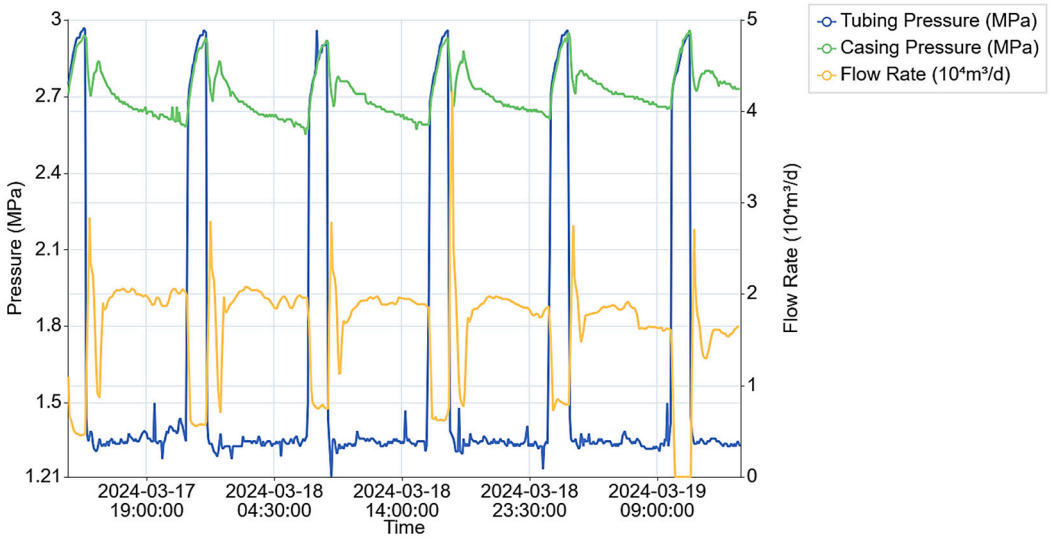


Figure 9. Instantaneous production curve of well opening model.

We have extracted actual daily production data from the oilfield's production database. Concurrently, we have generated predicted production data by integrating the transient production rates over time, as illustrated in Figure 9. These predictions are based on the theoretical model described in the manuscript. For a comprehensive comparison, we have juxtaposed the actual yields with the yields predicted by our model. The comparative results are meticulously organized and presented in Table 1, which features a clear and logical layout for ease of interpretation.

Table 1. Coupling results comparison table.

Case	Time	Production Model	Predicted Production (m^3/day)	Actual Production (m^3/day)	Forecast Error
Well A	3 December 2023	Produce for 3 h and shut-in for 5 h Three times a day	7382	7012	5.30%
Well B	4 December 2023	Produce for 3 h and shut-in for 3 h Four times a day	7228	8120	4.90%

In the realm of oil field extraction, the dynamism of well productivity stands as a pivotal determinant shaping the efficacy of the entire extraction process. Typically, during the initial stages of well initiation, a surge in productivity ensues owing to the release of subterranean reservoir pressure and the smooth flow of oil and gas. However, over time, a precipitous decline in well productivity becomes apparent, primarily driven by the attenuation of reservoir pressure and the decreasing yield of hydrocarbons. Once productivity wanes to a certain extent, the well's output stabilizes at a relatively subdued level, delineating a demarcation between high- and low-production phases.

In the pursuit of effectively managing well productivity and augmenting extraction efficiency, precise identification of peak-productivity epochs assumes paramount importance, facilitating the formulation of tailored extraction strategies. Techniques such as curve fea-

ture recognition serve as indispensable tools for parsing the evolving characteristics of well productivity curves, encompassing parameters like slope and inflection points. Through such analyses, high-productivity epochs can be discerned with relative accuracy. Subsequent to pinpointing these periods of peak productivity, interventions such as timely well closures can be implemented to preserve yields surpassing this threshold, thereby accruing energy reserves for subsequent well initiation endeavors, and consequently, enhancing the overall efficiency of oil field exploitation.

It is imperative to note that the determination of peak-productivity epochs is by no means a facile endeavor, necessitating meticulous scrutiny of copious production data. Owing to the intricacies and uncertainties inherent in subterranean reservoirs, peak-productivity epochs are subject to multifarious influences, demanding a holistic appraisal. In practical application, amalgamating mathematical models with computational algorithms facilitates an in-depth analysis of production data, engendering a more nuanced delineation of peak-productivity epochs, and concomitantly fostering the formulation of pertinent extraction strategies.

Specific methodologies predicated on curve feature recognition encompass segmenting instantaneous production curves into a succession of temporal windows, computing the mean production within each window, and subsequently, computing the range and minimum values within the new window sequence to encapsulate the evolving characteristics of the production curve. By stipulating a high-productivity coefficient, a threshold can be ascertained to demarcate high- and low-production phases, enabling the identification of the initial instance where production dips below this threshold as the peak-productivity epoch.

Employing time-window-based methodologies facilitates the identification of peak-productivity epochs, thereby assuming critical import in evaluating the duration of well initiation. Analyzing production curves enables the delineation of the temporal juncture wherein production commences a discernible descent, signifying the advent of low-productivity phases. Leveraging this metric allows for the calibration of well initiation durations to maximize production yields, effectuating the optimal management of well extraction, and striking a balance between resource utilization and production efficacy.

Figure 10 elucidates the impact of well opening and closure times on intermittent extraction, revealing variations in peak productivity and production time across different scenarios. Typically, in cases where reservoir properties are suboptimal, opening the well may lead to rapid energy depletion; hence, a reduction in well opening time can contribute to optimizing energy usage. In situations where productivity is high but production time is brief, adjusting the well opening time can enhance production efficiency. Conversely, when both productivity and production time are elevated, yet production duration is excessively brief, extending the well opening time may enable more comprehensive exploitation of latent production potential, representing an effective optimization strategy. In Figure 10, peak production time refers to the period from well opening until the point of demarcation between high and low production rates.

These optimization approaches offer a foundation for the development of strategies for the optimization of two wells. Precise calibration of well operation intervals, specifically the timing of well openings and closures, is essential for achieving an optimal balance. This balance is critical for maximizing oil and gas production while simultaneously ensuring the sustainable management of natural resources.

The optimization scheme of the two wells in Table 2 confirms the effectiveness and feasibility of the production guidance scheme provided.

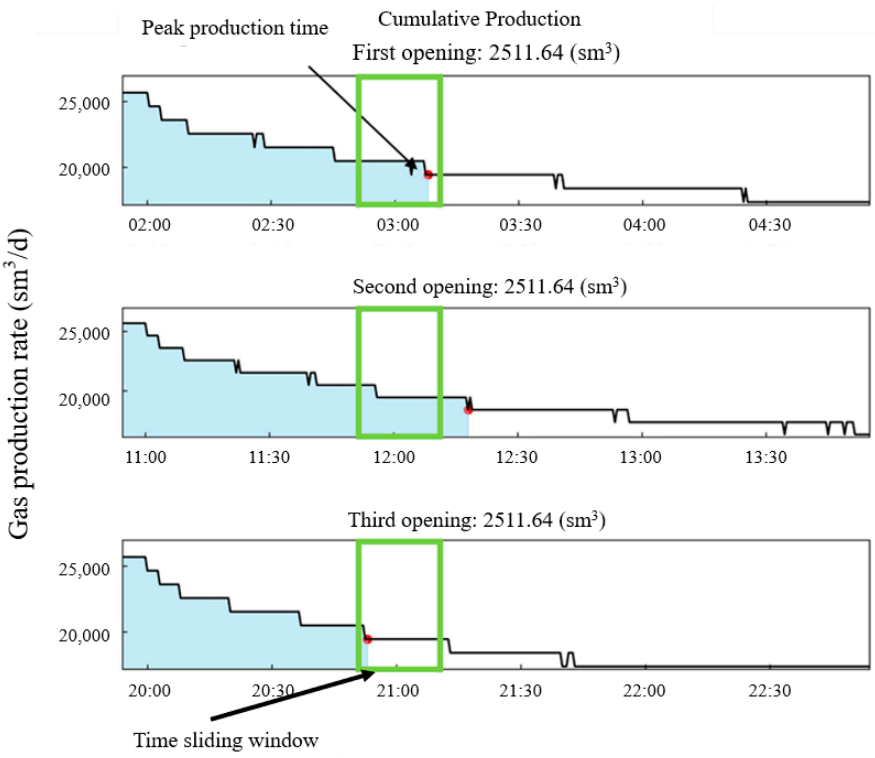


Figure 10. High-production time identification.

Table 2. Production guidance sheet.

Case	Production Model	Optimized Production Model	Production Suggestion
Well A	Produce for 3 h and shut-in for 5 h	Produce for 2 h and shut-in for 6 h	Reduce production time and improve shut-in time to reduce energy consumption during well opening.
Well B	Produce for 3 h and shut-in for 3 h	Produce for 4 h and shut-in for 3 h	Increase production time to increase gas production

4. Conclusions

(1) Through a stepwise approach involving the establishment of models for "gas well IPR prediction cased on wellhead test data analysis", "dynamic model for shut-in flowback stage", "wellbore flow model during well opening and liquid lifting stage", and a "reservoir–wellbore coupling model", an intermittent production optimization model tailored for the Changning block shale gas wells was developed.

(2) Within the comprehensive theoretical framework, several key challenges were addressed. The issue of high annular fluid levels during well opening was resolved, elucidating the drainage pattern of annular fluids. A method for identifying the elbow point was proposed, facilitating the calculation of casing shoe pressures.

(3) To tackle the problem of the ambiguity between pipeline pressure and flow rate, an iterative approach employing the nearest neighbor daily production as an initial estimate, coupled with a greedy algorithm for computing the closest neighboring production, was employed to mitigate convergence issues inherent in multiphase pipe flow.

(4) An optimization methodology for production systems was devised leveraging this theoretical foundation. This approach offers invaluable guidance for optimizing production regimes in well opening and closure operations.

Author Contributions: Conceptualization, Y.F. and G.H.; methodology, G.H.; software, J.C.; validation, G.H. and J.X. and C.Y.; formal analysis, Y.F.; investigation, C.Y.; resources, J.C.; data curation, J.C.; writing—original draft preparation, Y.F.; writing—review and editing, G.H.; visualization J.X.; supervision, G.H.; project administration, J.C.; funding acquisition, Y.F. All authors have read and agreed to the published version of the manuscript.

Funding: This research received no external funding.

Data Availability Statement: The original contributions presented in the study are included in the article, further inquiries can be directed to the corresponding author.

Conflicts of Interest: Authors: Yu Fan, Jiaxiao Chen, Jianhua Xiang, and Changqing Ye are employed by the PetroChina Southwest Oil & Gas Field Company. The remaining author declares that the research was conducted in the absence of any commercial or financial relationships that could be construed as a potential conflict of interest.

References

1. Johri, N.; Kadam, S.; Veeken, K.; Prakash, A.; Suvarna, H.; Singh, P.; Daukia, S.; Kadirus, S.; Goswami, A.; Aakash, S. Conquer Liquid Loading in Raageshwari Gas Field by Automated Intermittent Production and Deliquification. In Proceedings of the Abu Dhabi International Petroleum Exhibition and Conference, Abu Dhabi, United Arab Emirates, 2 October 2023.
2. van 't Westende, J.; van Nimwegen, D.; Belfroid, S.; Slot, H. Experiments of Liquid Loading and Intermittent Production Using a Lab-Scale Reservoir-Tubing Setup. In Proceedings of the SPE Annual Technical Conference and Exhibition, Abu Dhabi, United Arab Emirates, 15 September 2021.
3. Whitson, C.H.; Rahmawati, S.D.; Juell, A. Cyclic Shut-in Eliminates Liquid-Loading in Gas Wells. In Proceedings of the SPE/EAGE European Unconventional Resources Conference and Exhibition, Vienna, Austria, 20 March 2012.
4. Croce, D.D.; Zerpa, L.E. Intermittent Gas Lift for Liquid Loaded Horizontal Wells in Tight Gas Shale Reservoirs. In Proceedings of the SPE Artificial Lift Conference and Exhibition-Americas, Virtual, 10 November 2020.
5. Lee, J.; Wattenbargar, R.A. *Gas Reservoir Engineering*; Society of Petroleum Engineers: Kuala Lumpur, Malaysia, 1996; ISBN 978-1-61399-924-0.
6. Siripatrachai, N.; Shahkarami, A.; Zhang, J.; Tanner, S.; Reeves, B.; Kannappan, N.; Klenner, R.; Vianna, A.; Belyadi, H.; Patton, K. Active Learning Analytic Coupled with Edge Computing for Intermittent Shut-In Optimization and Carbon Emission Reduction in Shale Gas Reservoirs. In Proceedings of the SPE Annual Technical Conference and Exhibition, Abu Dhabi, United Arab Emirates, 15 September 2021.
7. Veeken, C.A. Best Practices to Predict and Recognize Liquid Loading and to Forecast and Maximize Intermittent Production. In Proceedings of the SPE EOR Conference at Oil and Gas West Asia, Muscat, Oman, 22 April 2024.
8. Wang, C.; Xiong, C.; Shi, J.; Han, Q.; Zhang, J.; Zhao, R.; Lei, G.; Zhang, X.; Sun, Y. A Method of Intelligent Scheme Optimization for Non-Stop System Intermittent Production Units. In Proceedings of the Abu Dhabi International Petroleum Exhibition and Conference, Abu Dhabi, United Arab Emirates, 11 November 2019.
9. Yu, T.T.; Zhang, H.-Q.; Li, M.X.; Sarica, C. A Mechanistic Model for Gas/Liquid Flow in Upward Vertical Annuli. In Proceedings of the SPE Annual Technical Conference and Exhibition, New Orleans, LA, USA, 4 October 2009.
10. Chen, Y.; Xie, Y.; Tian, W.; Wang, X.; Zhao, Z.; Xiao, S. Research on Intelligent Production Technology of Intermittent Gas Wells in Sulige Gas Field. In Proceedings of the International Petroleum Technology Conference, Virtual, 16 March 2021.
11. Gómez, J.F.; Omrani, P.S.; Belfroid, S.P.C. Data-Driven Optimization of Intermittent Gas Production in Mature Fields Assisted by Deep Learning and a Population-Based Global Optimizer. In Proceedings of the SPE Annual Technical Conference and Exhibition, Abu Dhabi, United Arab Emirates, 15 September 2021.
12. Caicedo, S. Estimating IPR Curves in Intermittent Gas Lift Wells from Standard Production Tests. In Proceedings of the SPE Latin America and Caribbean Petroleum Engineering Conference, Buenos Aires, Argentina, 25 March 2001.
13. Winterfield, C.D.; Missikos, J.; Tio, R.; Dalgety, B. Application of Closed Loop Control Logic to Optimise End-of-Life Cycling Production in a Mature Gas Field. In Proceedings of the SPE Asia Pacific Oil and Gas Conference and Exhibition, Adelaide, Australia, 14 October 2014.
14. Ye, C.; Tang, H.; Cai, D.; Xie, N.; Wang, Q.; Liu, J.; Jiang, L. Research on the Inflow Performance of the Plunger Lift in the Shale Gas Horizontal Well. *Math. Probl. Eng.* **2022**, *2022*, 4401128. [CrossRef]
15. Han, G.; Ma, G.; Gao, Y.; Zhang, H.; Ling, K. A New Transient Model to Simulate and Optimize Liquid Unloading with Coiled Tubing Conveyed Gas Lift. *J. Pet. Sci. Eng.* **2021**, *200*, 108394. [CrossRef]
16. Sukkar, Y.K.; Cornell, D. Direct Calculation of Bottom-Hole Pressures in Natural Gas Wells. *Trans. AIME* **1955**, *204*, 43–48. [CrossRef]

17. Correa, J.F.; Santos, O.G.; Inazumi, P.C.M. Intelligent Automation for Intermittent-Gas-Lift Oil Wells. In Proceedings of the SPE Latin America and Caribbean Petroleum Engineering Conference, Buenos Aires, Argentina, 25 March 2001.
18. Pestana, T.; Bordalo, S.; de Almeida Barreto Filho, M. Numerical Simulation in the Time Domain of the Intermittent Gas-Lift and Its Variants for Petroleum Wells. In Proceedings of the SPE Artificial Lift Conference-Latin America and Caribbean, Cartagena, Colombia, 21 May 2013.
19. Cadeño, M.; Ortiz, J.L. SOLAG: An Intelligent Gas Lift Optimization System for Continuous and Intermittent Gas Lift Wells. In Proceedings of the SPE Latin America and Caribbean Petroleum Engineering Conference, Buenos Aires, Argentina, 27 April 1994.
20. Gao, C.; Lee, W.J.; Spivey, J.P.; Semmelbeck, M.E. Modeling Multilayer Gas Reservoirs Including Sorption Effects. In Proceedings of the SPE Eastern Regional Meeting, Charleston, WV, USA, 8 November 1994.

Disclaimer/Publisher's Note: The statements, opinions and data contained in all publications are solely those of the individual author(s) and contributor(s) and not of MDPI and/or the editor(s). MDPI and/or the editor(s) disclaim responsibility for any injury to people or property resulting from any ideas, methods, instructions or products referred to in the content.